Single Element Thermal Sensor for Measuring Thermal Conductivity and Flow Rate inside a Microchannel

Non Peer-reviewed author version

OUDEBROUCKX, Gilles; NIEDER, Daniel; VANDENRYT, Thijs; BORMANS, Seppe; Möbius, Hildegard & THOELEN, Ronald (2021) Single Element Thermal Sensor for Measuring Thermal Conductivity and Flow Rate inside a Microchannel. In: SENSORS AND ACTUATORS A-PHYSICAL, 331 (Art N° 112906).

DOI: 10.1016/j.sna.2021.112906
Handle: http://hdl.handle.net/1942/34394

Single Element Thermal Sensor for Measuring Thermal Conductivity and Flow Rate inside a Microchannel

Gilles Oudebrouckx[a,b,1,*], Daniel Nieder[c,1], Thijs Vandenryt[a,b], Seppe Bormans[a,b], Hildegard Möbius[c], Ronald Thoelen[a,b]

[a] *UHasselt, Institute for Materials Research (IMO), Agoralaan, 3590 Diepenbeek, Belgium*
[b] *IMEC vzw, Division IMOMEC, Agoralaan, 3590 Diepenbeek, Belgium*
[c] *University of Applied Sciences Kaiserslautern, Department of Computer Sciences/Micro Systems Technology, Amerika Str. 1, 66482 Zweibrücken, Germany*

Abstract

The increasing development of continuous-flow applications in the field of microfluidics generates demand for in-line monitoring methods. The thermal conductivity (κ) of a liquid has been proven to be a valuable measurand for quality control, process monitoring, and analytical testing. However, most available methods for measuring κ of microliter-sized samples are limited for use on stagnant samples. In this work, a novel method and associated prototype device for measuring κ under flow conditions is presented. The so-called Transient Thermal Offset (TTO) method requires only a single metal resistive structure that is excitated with direct current (DC) pulses. To demonstrate the working, proof-of-principle experiments are performed on liquids with various κ under different flow rates. The results show that, after calibration, the presented microfluidic device can be used for accurately measuring κ of liquids under flow, as well as for determining the flow rate of liquids with a known κ. Within the explored ranges, both parameters can be determined with an average error of approximately 2.6%. The results confirm that, also under flow conditions, uncertainties concerning probing depth are eliminated with the TTO method.

*Corresponding author
Email address: gilles.oudebrouckx@uhasselt.be (Gilles Oudebrouckx)
[1] These authors contributed equally

Keywords: microfluidics, continuous-flow, thermal conductivity, flow rate
2021 MSC: 00-01, 99-00

1. Introduction

An accurate reading of thermal conductivity (κ) can reveal more about a liquid sample than only its ability to conduct heat. Measurements of κ can be used for quality control, process monitoring, and analytical testing. For example it is possible to use a value of κ to estimate the ratio of two mixed liquids [1, 2], the concentration of cell suspensions [3], and the presence or size of nanoparticles in suspension [4, 5]. In applications where the sample liquid is costly or scarcely available, it is often desired to perform such thermal measurements inside a microfluidic device. Fortunately, literature offers various methods for measuring the thermal conductivity of microliter-sized samples. However, most available methods are limited for measurements on stagnant fluids.

Because of recent developments in continuous-flow microfluidics, it is becoming more expedient to be able to measure κ under flow conditions. Possible applications are for in-line monitoring of mixing [6], for monitoring the continuous-flow separation of cells and particles [7, 8, 9], or for monitoring cell cultivation and proliferation under flow conditions inside a microfluidic device [10, 11, 12].

Most common methods for measuring κ inside a microchannel require a separate heating and temperature sensing element for measuring the temperature drop between two positions inside the microchannel. Generally, heating is achieved via a resistive heating element [13, 14], whereas temperature sensing is done with thermocouples [13, 14, 15]. Alternatively, there are also methods available that only require a single metal resistive element for determining κ such as the hot strip method [16, 17] or the 3ω method [18]. Single-element methods offer a simple sensor construction. However, they also have disadvantages. With the previously mentioned single-element methods, uncertainties can arise concerning the thermal

probing depth [19, 20, 21]. If the probing depth exceeds the boundaries of the sample, the measurement will be disturbed by the surrounding material. This can be challenging when working with microliter-sized fluid samples. With fluid samples under flow, it becomes even more difficult to estimate the thermal probing depth. Furthermore, with alternating current (AC) based single-element methods, such as the 3ω method, the required read-out hardware and the corresponding data analysis is more complex as compared to direct current (DC) based single-element methods, such as the hot strip method [16, 20].

For quantifying the flow inside a microchannel, many sensing options are available. Various microelectromechanical system (MEMS) flow sensors exist, which incorporate a moving structure such as a cantilever [22], spring [23] or diaphragm [24]. However, most common methods for measuring flow rate are thermal-based, whereby very similar sensors are used as described above for measuring κ. Using a separate heating and temperature sensing element, the time-of-flight principle can be applied. Hereby the time required for a thermal pulse to travel from heater to sensor is recorded and used as an indicator for flow speed. With single-element thermal sensors, the additional cooling of the heater caused by heat transfer due to mass transfer can be used to measure flow rate [25, 26].

This current study builds on our previous work, in which we have developed a method and associated device for measuring κ of microliter-sized samples with a high accuracy of 0.5% [27]. With this transient, single-element method, issues concerning probing depth were eliminated. So far, the research was limited to measurements on stagnant liquids inside the microchannel. In this work, the aim is to investigate the ability to measure κ under continuous flow conditions to demonstrate the possibility of in-line monitoring of κ. Also, the sensor's ability to measure flow rate of fluids with a known κ is assessed.

2. Working Principle

Fig. 1a shows a schematic cross-section of the microfluidic device. The bottom of the microchannel consists of a thin substrate on which a metal meander structure is deposited. The top of the microchannel is made of aluminium. The material choice for aluminium is made specifically for its high thermal conductive properties, as discussed later.

During measurements, the metal structure is used as a Joule heating element by applying a current pulse, similarly to the conventional hot strip method [17, 28]. The temperature rise of the metal structure will cause an increase in the electrical resistance of the metal structure itself, as determined by Eq. (1). By simultaneously measuring voltage whilst applying the heating current, it is possible to measure this change in electrical resistance. By doing so, the metal structure can simultaneously be used as a heating element, as well as a temperature sensor for measuring the sensor temperature response to a heating step.

$$R = R_{ref}[1 + \alpha(T - T_{ref})] \tag{1}$$

where:

R = electrical resistance of structure [Ω]
T = temperature of structure [K]
R_{ref} = electrical resistance at temperature T_{ref}
α = temperature coefficient of resistance [1/K]

The traditional hot strip principle prescribes that the probing depth of the applied thermal pulse can not exceed the boundaries of the sample under measurement [21, 28, 29]. On this condition, the principle states that the sensor temperature response will approach linearity when plotted versus the square root of time, with a slope that is inversely related to the thermal

effusivity (e) of the sample [21, 28, 29]. In case of an excessive probing depth, the measured slope will be disturbed by the surrounding material [16].

The novelty of the presented device is in the crucial role of the aluminium top piece for the readout to eliminate uncertainties concerning the probing depth. As illustrated by the red arrows in Fig. 1a, we intentionally apply thermal pulses that probe beyond the physical boundaries of the liquid inside the microchannel. The aluminium top is a good heat conductor which acts as a heat sink to absorb heat dissipated by the sensor structure. For the principle to work, the aluminium top piece must be significantly thicker than the height of the microchannel, so that during a heating step the piece can be considered as a semi-infinite medium [28]. In this case, the expected sensor temperature response can still be described by the hot strip principle. When heating sufficiently long, the sensor temperature response should approach linearity when plotted versus the square root of time, with a slope that is determined by e of the aluminium top piece [21, 28, 29]. This implies that the end of all sensor temperature responses are expected to be parallel, regardless of the thermal properties of the fluid inside the microchannel. This expected sensor response was confirmed in our previous work [27]. More interestingly, in this earlier work, we found that the offset on this linear part of the sensor response can be used to measure κ of the liquid, as illustrated in Fig. 1b. Via a Cauer-type thermal equivalent circuit of the sensor, numerical simulations, as well as with practical experiments, it was demonstrated that only κ of the liquid affects the offset, without influence from the density or specific heat capacity of the liquid [27]. Thus, contrary to the traditional hot strip method, κ of the sample is not derived from the slope measured inside the sample, but rather from the offset measured inside a high thermal conductive reference material on top of the sample. Hence the name Transient Thermal Offset (TTO) method. The constant measured slope at the end of the sensor response acts as confirmation that the probing depth is sufficient. Thus, all uncertainties concerning probing depth are removed. However, so far, only measurements were performed on fluids that were stagnant inside the microchannel.

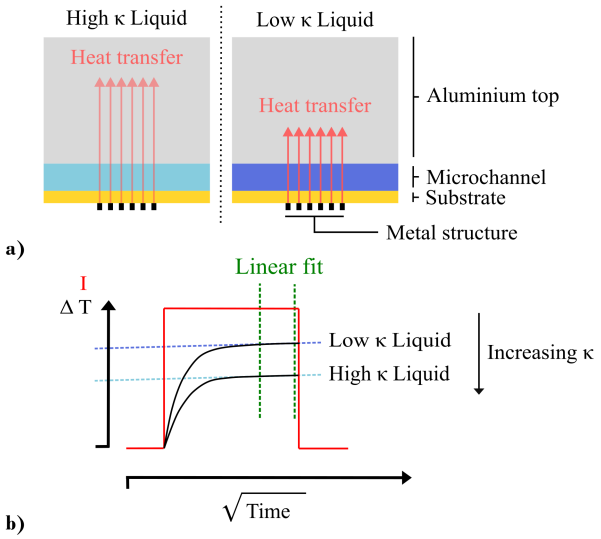

Figure 1: **a)** A schematic cross-section of the microfluidic device during measurements on stagnant liquids with a different thermal conductivity (κ). The heat generated by the metal structure will propagate through the liquid inside the microchannel into the aluminium top material. A liquid with a low κ will act as a thermal barrier, impeding heat transfer towards the aluminium top. **b)** Generic temperature response curves illustrated based on the Cauer-type thermal equivalent circuit of the sensor device presented in our previous work [27]. In this earlier work, it was demonstrated that the offset of a linear regression at the end of a sensor response curve can be used to determine κ of stagnant liquids inside the microchannel.

In measurements, where a stagnant fluid is inside the microchannel, heat transfer only occurs via thermal conduction. Moreover, the heat transfer occurring near the sensor can be approximated as being one-dimensional (1D) due to the sensors geometry and device construction [14, 27]. In the case of measuring flowing liquids, however, additional heat transfer will occur via heat transfer due to mass transfer. As illustrated in Fig. 2a, we expect that this additional heat transfer will reduce the sensor temperature response. More specifically, the expectation is that the measured offset will decrease as the flow rate increases. This research investigates whether this effect can be exploited for performing flow rate measurements of liquids with a known κ.

Demonstrating this possibility would also imply that measuring κ of liquids at a known flow rate is possible.

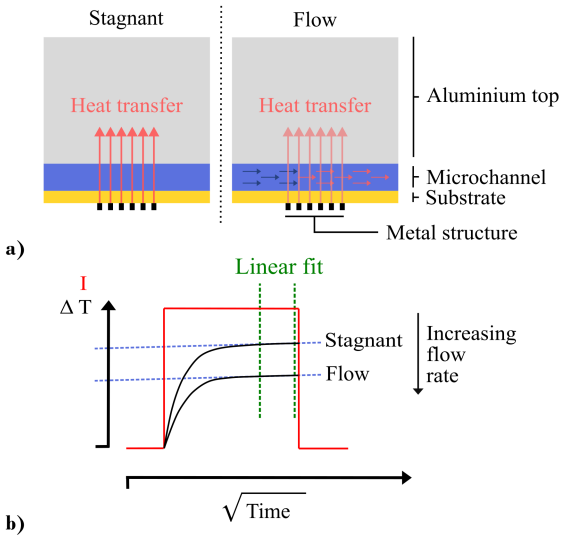

Figure 2: **a)** A schematic cross-section of the microfluidic device during measurements on a liquid under stagnant and flow conditions. In the case of a flowing liquid, additional heat transfer will occur via heat transfer due to mass transfer. **b)** We expect that the additional heat transfer will lower the sensor temperature response. In this work, we will investigate the influence of mass flow on the sensor temperature response in an effort to measure flow rate as well as to measure κ of liquids in flow.

3. Materials and Methods

First, the build-up of the microfluidic device is discussed. Second, the overall measurement setup is presented, including the used readout device and the pump setup used for measuring liquids under flow. It should be noted, however, that the build-up of the sensor device and the overall measurement setup are identical as described in our earlier work on stagnant fluids [27]. Lastly, the measurement procedure is explained.

3.1. Microfluidic Device

The sensor structure was designed in-house and fabricated externally (PCBWay, China) on a flexible Printed Circuit Board (PCB) as shown in Fig. 3a. The substrate is a 40 μm thick polyimide film. The meander-shaped gold-coated copper structure, schematically illustrated in Fig. 3c, is 5 mm $\times$ 1.3 mm in scale. The meandering tracks have a width and spacing of 60 μm and a height of 15 μm. To measure the initial electrical resistance of the structures at room temperature (R_{init}), a limited current of 10 mA is used to prevent Joule heating. The R_{init} of different sensors varies between 1.8 Ω and 2.3 Ω. The temperature coefficient of resistance was determined experimentally ($\alpha = 3.448 \times 10^{-3} \pm 0.033 \times 10^{-3}$ K^{-1}).

The microfluidic channel, shown in Fig. 3a, is designed and fabricated in-house. The channel has rounded outlines to counteract the accumulation of air bubbles. The shape is cut out of a 130 μm thick sheet of Parafilm M®. This sheet is then carefully aligned on top of the flexible PCB. The metal structure must be facing down in order that the polyimide substrate is present between the metal structure and the liquid inside the microchannel. This is necessary to prevent electrical shorts due to direct contact between the liquid and the metal. It should be noted that the rheological behavior of non-Newtonian fluids was not considered during the design of this microchannel. It is known that, as the shear rate increases, κ of non-Newtonian liquids increases [30]. However, the experimental part if this study is limited to Newtonian fluids, of which the thermal conductivity is independent of shear rate. Nevertheless, it is possible to implement the TTO mesurement principle into differently shaped microchannels, optimized for specific applications with non-Newtonian liquids.

The aluminium top piece, shown in Fig. 3b, is 10 mm thick, and is thus over 75 times thicker than the height of the microchannel. The piece is fabricated externally (YouniQ, Belgium). The sensor and microchannel are placed on this piece of aluminium. Next, the Parafilm M® is heat-sealed between the aluminium and the sensor substrate, as suggested by Wang et al. [27, 31].

Screw-type connectors for the inlet and outlet of the microchannel are machined directly into the aluminium.

To provide a rigid back support, a polymethyl methacrylate (PMMA) plate is added to the backside. As an extra precaution to prevent the flexible PCB from bending, a piece of double-sided tape is added (Fig. 3b), which prevents the flex PCB from moving. Finally, all components are screwed together. As shown in Fig. 3d, the transparent backplate allows for visual inspection of the content of the microchannel.

As the height of the microchannel is equal to the thickness of the Parafilm M®, we calculate that the elliptic cylindrical fluid column surrounding the sensor, marked in Fig. 3c, has a volume of 2.76 μl. During measurements on stagnant fluids, heat transfer within this region can be approximated as being one-dimensional due to the microchannel aspect ratio (height/width) [14, 27]. Therefore, with stagnant measurements, we consider this to be the volume of the liquid under test.

3.2. Experimental Setup

The overall measurement setup is depicted in Fig. 4. To perform the 4-wire measurement as described in Section 2, a 4-wire Source Measure Unit (SMU) is used. More specifically, a PXIe-4139 Precision SMU (National Instruments) is used in combination with the PXIe-1073 Chassis (National Instruments). The SMU is controlled by a custom LabVIEW program in which the properties of the thermal pulses can be configured. For all presented experiments, identical constant current heating pulses are applied continuously throughout the measurement. The pulses, measured at 100 Hz, have a power of approximately 0.30 W and a duration of 16 s [27]. Each heating step is followed by a cool-down period of 84 s. The cool-down period is more than sufficiently long to allow the sensor to cool down back to ambient temperature before each new thermal pulse. With the previously mentioned heating duration and power, cool-down periods of 20 s are sufficient to cool down fully to ambient temperature when water is inside the microchannel. However, the

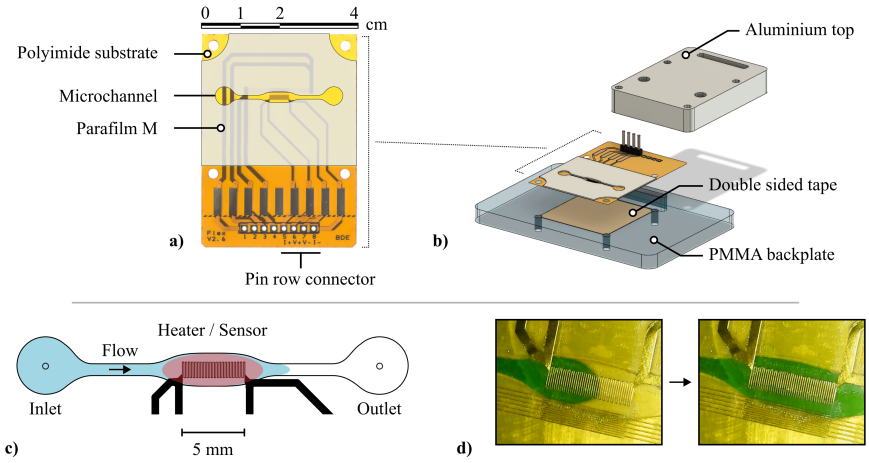

Figure 3: An overview of the build-up of the sensor device [27]. **a)** A picture of the flexible PCB on which the sensor structure is present. The microchannel around the sensor structure is fabricated out of Parafilm M. **b)** The flexible PCB and the microchannel are sandwiched between the aluminium top and a rigid PMMA backplate. Before adding the backplate, the Parafilm M is sealed between the PCB and the aluminium. **c)** A schematic illustration of the sensor structure and the microchannel. The marked elliptic cylindrical fluid column, which we consider to be the measurement volume in stagnant measurements, has a volume of 2.73 μl. **d)** Close up pictures of the microchannel taken while a blue-colored liquid is flushed in. The transparent PMMA backplate and transparent polyimide substrate allow for visual inspection of the content of the microchannel.

time of 84 s is required to refill the syringe pump used to apply constant flow rates, as discussed later. By letting the sensor cool down to ambient temperature in between pulses, it is possible to use the sensor structure as a Resistive Temperature Device (RTD) to monitor the temperature of the liquid. Doing so can prevent misinterpretations of the data due to variations in the liquid temperature.

The required current for applying the power of 0.30 W is dependent on the R_{init} of the sensor. Therefore, before each measurement, R_{init} is measured, and the required heating current (I) for each individual sensor is calculated using

the power equation, Eq. (2).

$$I = \sqrt{P/R_{\text{init}}} \tag{2}$$

where:

I = sensor specific heating current [A]
P = desired heating power [W]
R_{init} = initial resistance [Ω]

A programmable syringe pump (LSPone, Advanced Microfluidics) is used for flushing in and replacing liquids inside the device as well as for creating a constant flow rate for non-stagnant measurements. As shown in Fig. 4, the pump is equipped with an 8-channel rotary valve. This allows us to automatically flush fluids from different sample containers. The total volume of the glass syringe is 1 ml. Given that the maximum used flow rate during experiments is 20 μl/s, the syringe is empty after 50 s of pumping. Therefore, the SMU control was synchronized with the pump control to ensure that refills only occur during the cool-down periods.

All presented measurements have been performed in a temperature-controlled room (20 °C ± 1 °C). The used liquid mixtures were made in advance and stored inside the same room to ensure that all liquids were at room temperature prior to measuring.

3.3. Measurement Procedure

To check the influence of mass flow rate on TTO measurements, initially, measurements on purified water (Sartorius) at various flow rates are performed. Hereby each experiment exists out of three sequential stages, each with a duration of approximately 25 min. First, stagnant water is present inside the microchannel whilst the thermal pulses are applied. Secondly, water is flushed at a constant flow rate. Thirdly, and finally, measurements are performed under stagnant conditions again. This measurement protocol allows us to compare the sensor temperature response curves under flow, with curves

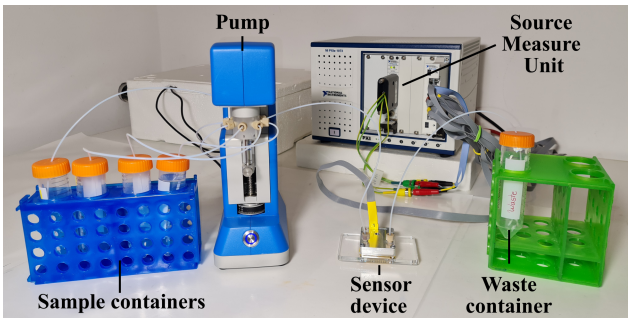

Figure 4: A picture of the overall measurement setup. The automated syringe pump is used for flushing liquid samples through the sensor device. Meanwhile, thermal pulses are simultaneously applied and measured using a source measure unit.

measured in the stagnant stages preceding and succeeding the flow stage. We will investigate the percentage change in offset under flow relative to offset measured on stagnant water [27]. This protocol is done using the following flow rates for the second measurement stage: 0 (stagnant), 5, 10, 15, and 20 μl/s. For data processing, the time interval for the linear fit is chosen to be [2.4, 4] $s^{1/2}$, identical as in earlier work [27]. This corresponds with a time interval between 5.76 s and 16 s.

To investigate the influence of κ of the liquid on flow rate measurements and to explore the possibility to measure κ of liquids under flow, the measurement procedure was altered. Instead of only using purified water, also liquids with a different thermal conductivity are used. More specifically, ethanol absolute ($\geq$99.8%) (VWR Chemicals, Belgium) and a 50 vol% water/ethanol mixture are used for the second measurement stage. Ethanol is chosen because of its significant difference in κ as compared to water. The κ values of water and ethanol were taken from literature [32]. For the 50 vol% water/ethanol mixture, κ was calculated using the rule of mixtures [33, 34]. The κ values of all used liquids are listed in Table 1. For the stagnant measurement stages, water was still used as a measurement liquid. This way, stagnant water remains the reference condition to which other values of offset will be compared. This protocol is done using identical flow rates for the

second measurement stage as mentioned earlier: 0 (stagnant), 5, 10, 15, and 20 μl/s.

Liquid [**vol% ethanol**]	$\boldsymbol{\kappa}$ [**W/mK**]
0 (pure water)	0.603
50	0.392
100 (pure ethanol)	0.180

Table 1: Values of thermal conductivity (κ) of used liquids, as found in literature [32].

4. Results and Discussion

Experiments are performed as described in Section 3.3. Initially, measurements are performed on water in order to investigate the influence of flow rate on TTO measurements. Next, the experiments are repeated with pure ethanol and a 50 vol% water/ethanol mixture for the non-stagnant part of the measurement procedure. This data is then used to investigate the influence of κ on flow rate measurements. Finally, the sensor's ability to measure κ of liquids in flow is discussed.

4.1. Influence of Flow Rate on TTO Measurements in Water

As mentioned in Section 3.3, the measurement procedure contains three steps, each with a duration of 25 min. During the first and last step, stagnant water is present inside the microchannel. In between the second step, different flow rates are applied. All resulting changes in voltage, measured as a response to the applied thermal pulses, are plotted over each other in Fig. 5a. The raw data in this figure shows that that all measured sensors response curves are parallel at the end. From this we conclude that, also under flow conditions, it is possible to probe beyond the physical boundaries of the liquid inside the microchannel, into the aluminium top. Therefore, we confirm that, also under flow conditions, uncertainties concerning probing depth are eliminated with

the TTO method. Furthermore, from Fig. 5a, we can derive that the offset at the end of the curve is influenced by the flow rate of the fluid inside the microchannel. This is clear because all voltage curves measured under stagnant conditions are grouped, whereas the voltage curves measured under flow conditions decrease as the flow rate increases. These voltage curves can be converted to temperature using Eq. (1). After doing so, we find that the temperature of the sensor structure increases with 1.5 K in stagnant water, and only 1.0 K when the water flows at 20 μl/s.

To inspect the change in offset at the end of the transient curves more closely, linear regression is performed on each individual voltage curve within the time interval of 2.4 $s^{1/2}$ to 4 $s^{1/2}$ (Fig. 5a). Next, the offsets of the regression lines are plotted as a function of the start time of the applied heating curve. More precisely, the percentage change in offset is plotted as compared to the offset measured under stagnant conditions (Fig. 5b). This plot clearly shows the three different measurement stages. The period between 30 min and 50 min is marked as the flow interval.

A small spike in offset is present in the middle of the flow period of the 15 μl/s measurement. This spike could be there due to the presence of a small air bubble inside the microchannel during flow. Air has a very low κ (0.025 W/mK) [32], and therefore, a small air bubble can cause an increase in offeset [27]. Therefore we suspect that unwanted air bubbles are the most common cause for deviations in TTO measurements.

Finally, all data points within the flow period, as marked in Fig. 5b, are plotted as a function of the applied flow rate, see Fig. 5c. This plot clearly shows the significant changes in offset caused by variations in flow rate. Furthermore, from this plot, we conclude that the relation between flow rate and the change in offset is linear within the explored range of 0 μl/s to 20 μl/s.

With the currently used measurement configuration, heating steps of 16 s were applied, followed by cooling periods of 84 s. Hence, the measurements in Fig. 5b contain one data point every 100 s. However, as mentioned in Section 3.2, the cool-down duration can be reduced greatly. A visual

inspection of Fig. 5a suggests that also the heating duration can be shortened by at least several seconds since a more narrow and earlier regression interval would return similar offset values. By reducing the duration of the heating and cooling period, the overall measurement speed can be increased significantly. An even further reduction in the required heating time can be achieved by reducing the height of the microchannel [27].

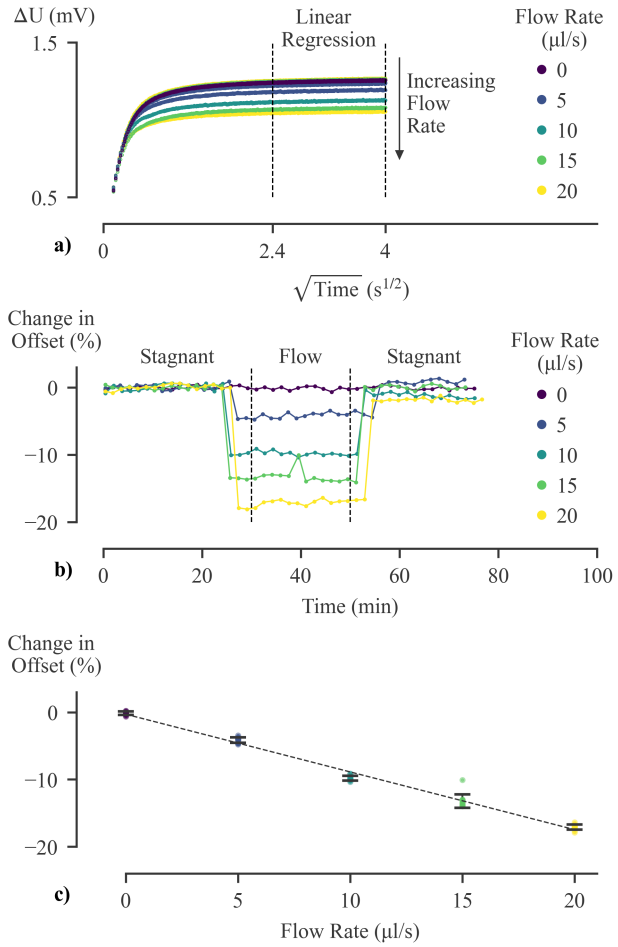

Figure 5: **a)** Measurements were performed as explained in Section 3.3. All voltage curves measured as a response to a heating pulse are plotted over each other. The raw data suggests the sensor temperature response indeed is influenced by the flow rate of the liquid. For closer analysis, linear regression was performed on each individual voltage curve within the marked time interval. **b)** The percentage change in the offset of the obtained linear regression is plotted as a function of time. **c)** All offset values obtained during the flow interval, between minute 30 and 50, are plotted as a function of the applied flow rate. We conclude that there is a linear relationship between the measured offset and the flow rate of the liquid inside the microchannel.

4.2. Measuring Flow Rate of Liquids with Different Thermal Conductivity

The sensor's ability to measure flow rate was confirmed in Section 4.1. In this subsection, we will discuss the influence of κ of the liquid on flow rate measurements. Therefore, as mentioned in Section 3.3, the experiments presented in Fig. 5 were repeated with two liquids with a different κ for the flow part of the measurement. For the stagnant stages, again water was used. As described in Section 4.1, linear regression was performed at the end of the voltage curves, and all measured changes in offset, relative to stagnant water, are plotted as a function of the applied flow rate in Fig. 6a. Note that the data for 0 vol% ethanol (pure water) in this graph is the same exact data as plotted in Fig. 5c.

The data shown in Fig. 6a shows that also the flow rate of liquids with a lower κ can be measured. Moreover, within the explored range of 0.180 W/mK to 0.603 W/mK, the relationship between offset and flow rate is linear. However, it is important to point out that the linear regression lines visible in Fig. 6a are not parallel. More precisely, the slope of the regression line becomes less steep with increasing κ. Consequently, for a liquid with a low κ, a given increase in flow rate will have a more significant impact in reducing the sensor temperature response as compared to a liquid with high κ, for which the sensor temperature response is already low under stagnant conditions.

Using the linear regressions in Fig. 6a, all offset values are converted to a value of flow rate. These converted values are called the measured flow rate from now on. The configured flow rate of the pump is considered to be the actual flow rate. In Fig. 6b, the measured flow rate values are plotted as a function of the actual values of flow rate. This plot clearly shows the sensor's ability to measure the absolute flow rate of liquids with different κ, provided that the two following conditions are met. Firstly, κ of the fluid under measurement should be known. Secondly, the necessary regression lines to convert offset values to flow rate need to be available for fluids with that particular κ value.

An overview of the measured flow rates, the accuracy, and the precision is given in Table 2. On average, the flow rate measurements have an accuracy of

2.6% and a standard deviation of 2.04 μl/s. As mentioned before in Section 4.1, also for measurements on flowing liquids, uncertainties concerning probing depth are eliminated via the TTO measurement principle.

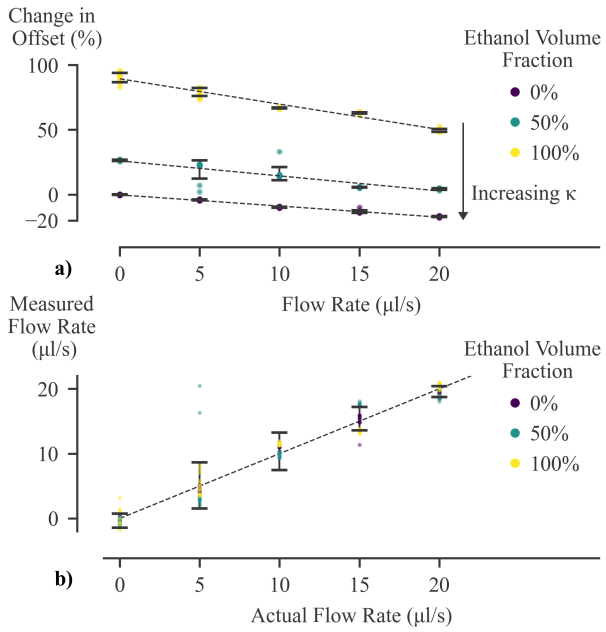

Figure 6: **a)** The measurement procedure is performed with pure water, pure ethanol, and a 50 vol% dilution. The percentage changes in offset for each liquid are plotted as a function of the applied flow rate. Linear regressions made for each liquid suggest that offset decreases linearly as the flow rate increases. However, the relation between both is steeper for liquids with a low κ. **b)** Using the linear regressions, the values for the percentage change in offset are converted to a measured flow rate value. The measured flow rates are compared with the actual flow rate to which the pump is configured. This plot confirms the sensor's ability to measure the flow rate of liquids with different κ

4.3. Measuring Thermal Conductivity in Flow

In the Section 4.2, we discussed the sensor's ability to measure the flow rate of liquids with various κ. The data presented in that section will now be processed in an alternative manner in order to investigate the sensor's ability to measure κ of liquids under flow.

Acutal Flow Rate [μl/s]	**Mean Measured Flow Rate [μl/s]**	**Accuracy [%]**	**Standard Deviation [μl/s]**
0	-0.35	-	1.10
5	5.10	2.0	3.57
10	10.35	3.5	2.88
15	15.39	2.6	1.81
20	19.56	2.2	0.84
	Average	**2.6**	**2.04**

Table 2: Accuracy and precision of flow rate measurements on liquids with different thermal conductivity (κ).

In Fig. 7a, the offset data of experiments presented earlier, in Fig. 6a, is plotted as function of the κ of the used liquid (Table 1). In a previous study, in which only measurements on stagnant liquids were performed, we found that the relation between the percentage change in offset and the κ of the liquid can be approximated with an exponential equation of the form $y = a + b \cdot e^{-cx}$. For the specific design of the sensor used in this work, $a = -29.8, b = 240$, and $c = 3.43$ [27]. This specific exponential equation represents the original calibration curve, shown in Fig. 7a.

As expected, all data points measured under stagnant conditions can be found on or near this calibration curve (Fig. 7a). However, changes measured in offset during flow significantly deviate from the original calibration curve. As shown in Fig. 7a, under flow, the measured offsets are lower than expected from the stagnant calibration curve. The relationship between κ and changes in offset measured under flow can be approximated by shifting the original calibration curve. For doing this, two new coefficients are added to the original calibration curve: $y = (a - v) + b \cdot e^{-c(x-h)}$. By using a, b, and c mentioned earlier, only the two new coefficients v and h needed to be found for each flow rate using regression analysis. The obtained calibration curves, corrected for flow rate, are shown in Fig. 7a. An overview of the obtained v and h coefficients are listed in Table 3.

Using the regression lines presented in Fig. 7a, all measured changes in offset are converted to a value of κ. In Fig. 7b, the measured κ values are plotted as a function of the actual κ of the fluid (Table 1). From this plot it is clear that accurate measurements of κ under flow are possible. The average accuracy within the demonstrated range of 0 μl/s to 20 μl/s, is 2.50 %, and the standard deviation is 0.018 W/mK. A detailed overview of the accuracy and precision of κ measurements is given in Table 4.

Flow rate [μl/s]	**Coefficient v**	**Coefficient h**
0	0	0
5	1.625802	-0.04786253
10	2.928464	-0.0759601
15	9.699794	-0.07152078
20	7.805258	-0.1156289

Table 3: Value for coefficients v and h for exponential fit.

It has been demonstrated that measuring flow rate of liquids with known κ, as well as measuring κ of liquids under a known continuous flow rate is possible with the presented device. This implies that it is possible to achieve both functions simultaneously by incorporating two identical sensing structures into a two-branch microchannel. Additionally it is required that the flow in one channel can be stopped by a controllable valve. This way, a stagnant measurement of κ can be performed in one channel. This measured κ value can simultaneously be used for the deriving the flow rate from the measurement in the channel with flow. By periodically opening and closing the valve, the liquid inside the stagnant channel can be refreshed. A similar approach was suggested by Offenzeller et al. for their implementation of a κ sensor, and time-of-flight based flow sensor inside a microchannel [35].

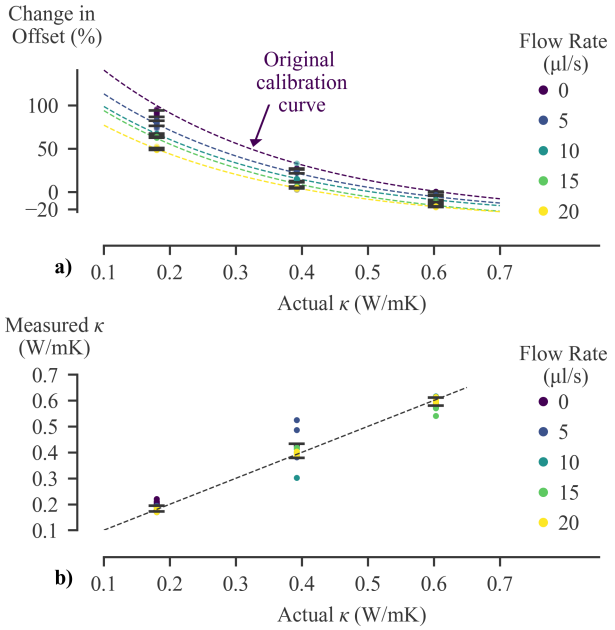

Figure 7: **a)** Offset values are plotted as a function of the thermal conductivity of the fluid as found in literature. As demonstrated earlier for stagnant fluids, the relationship between changes in offset and κ can be approximated with an exponential equation: the original calibration curve [27]. With increasing flow rate, the original calibration curve can be shifted down and left to approximate the relation between changes in offset and κ. **b)** The offset values are converted to measured values of κ using the exponential equations. When comparing the measured κ values with the actual κ values, it is clear that measurements of κ are possible on liquids under flow.

Liquid [vol% **ethanol**]	**Actual** κ [**W/mK**]	**Mean Measured** κ [**W/mK**]	**Accuracy** [%]	**Standard Deviation** [**W/mK**]
0 (pure water)	0.603	0.596	1.2	0.015
50	0.392	0.406	3.6	0.027
100 (pure ethanol)	0.180	0.185	2.8	0.011
		Average	**2.5**	**0.018**

Table 4: Accuracy and precision of thermal conductivity (κ) measurements of liquids under flow.

5. Conclusion

The in-house developed microfluidic device used in this study was originally designed to measure thermal conductivity (κ) of stagnant liquids inside a microchannel with the Transient Thermal Offset (TTO) method. The purpose of this research was to investigate the influence of flow rate on TTO measurements. Firstly, this was done to explore the possibility of measuring flow rate with the TTO method. Secondly, to investigate the accuracy of κ measurements on flowing liquids inside a microchannel.

The results of this investigation show that both new suggested applications are possible. Measuring flow rate is possible, provided that κ of the liquid is known, and the specific linear calibration curve for a liquid with this κ value is available. This calibration curve is used for converting measured offset values to flow rate for liquids with that particular κ value. Within the demonstrated flow range of 0 μl/s to 20 μl/s, and for fluids with κ ranging between 0.180 W/mK and 0.603 W/mK, the measured flow rates have an average standard deviation of 2.04 μl/s and accuracy of 2.6%.

Measuring absolute values of κ of liquids under continuous flow can be done, given that the flow rate is known and the specific exponential calibration curve is available. The data showed that, also under flow conditions, uncertainties concerning the thermal probing depth are eliminated with the TTO method. Within the explored ranges, the κ measurements have an average standard deviation of 0.018 W/mK and accuracy of 2.5%. This measurement principle can be of value for in-line monitoring of continuous-flow microfluidic applications. Examples of such applications include the mixing of fluids, continuous-flow separation of cells and particles, and cell proliferation in flow conditions. The current research, however, is limited by the use of Newtonian fluids. When exploring applications with non-Newtonian fluids, such as cell suspensions, it is important to take into account the influence of shear rate on thermal conductivity. For this reason, it can be opportune to integrate the sensing principle in a differently shaped

microchannel that is optimized for a specific application.

Suggestions were made to improve the measurement speed of the presented device specifically, by shortening the heating and cooling periods. Since the measurement principle can also be integrated into smaller microchannels, even further improvements in measurement speed are possible. The before-mentioned applications of measuring flow rate and κ can also be incorporated in one single device for simultaneous monitoring of both measurands. To do so, a two-branch microchannel needs to be developed that contains an identical sensing element in each of the two branching channels. Additionally, a controllable valve needs to be integrated in one of the two channels to allow for a stagnant measurement of κ.

Acknowledgment

The authors acknowledge the financial support by the DAAD (German Academic Exchange Service) through the project MPFL - Meeting Point Functional Layers.

References

[1] U. Gaitonde, D. Deshpande, S. Sukhatme, The thermal conductivity of liquid mixtures, Industrial & Engineering Chemistry Fundamentals 17 (4) (1978) 321–325.

[2] M. Ortiz, N. Gonzales, C. Guzman, E. Paiva, E. Bello, Thermal conductivity of mixtures, in: Thermal Conductivity 18, Springer, 1985, pp. 213–223.

[3] B. K. Park, N. Yi, J. Park, Y. Kim, D. Kim, Development of a thermal sensor to probe cell viability and concentration in cell suspensions, AIP Advances 4 (4) (2014) 047120.

[4] S. Pil Jang, S. U. Choi, Effects of various parameters on nanofluid thermal conductivity, ASME Journal of Heat Transfer.

[5] M. Chopkar, S. Sudarshan, P. Das, I. Manna, Effect of particle size on thermal conductivity of nanofluid, Metallurgical and materials transactions A 39 (7) (2008) 1535–1542.

[6] C.-Y. Lee, C.-L. Chang, Y.-N. Wang, L.-M. Fu, Microfluidic mixing: a review, International journal of molecular sciences 12 (5) (2011) 3263–3287.

[7] N. Pamme, Continuous flow separations in microfluidic devices, Lab on a Chip 7 (12) (2007) 1644–1659.

[8] M. Wu, A. Ozcelik, J. Rufo, Z. Wang, R. Fang, T. J. Huang, Acoustofluidic separation of cells and particles, Microsystems & nanoengineering 5 (1) (2019) 1–18.

[9] J.-H. Lee, S.-K. Lee, J.-H. Kim, J.-H. Park, Separation of particles with bacterial size range using the control of sheath flow ratio in spiral microfluidic channel, Sensors and Actuators A: Physical 286 (2019) 211–219.

[10] M. Tehranirokh, A. Z. Kouzani, P. S. Francis, J. R. Kanwar, Microfluidic devices for cell cultivation and proliferation, Biomicrofluidics 7 (5) (2013) 051502.

[11] W. E. Svendsen, J. Castillo-Leon, J. Lange, L. Sasso, M. H. Olsen, M. Abaddi, L. Andresen, S. Levinsen, P. Shah, I. Vedarethinam, et al., Micro and nano-platforms for biological cell analysis, Sensors and Actuators A: Physical 172 (1) (2011) 54–60.

[12] K. Sato, M. Sato, M. Yokoyama, M. Hirai, A. Furuta, Influence of culture conditions on cell proliferation in a microfluidic channel, Analytical Sciences (2018) 18SDP04.

[13] C. Offenzeller, M. Knoll, T. Voglhuber-Brunnmaier, W. Hilber, B. Jakoby, Screen printed sensor design for thermal flow velocity measurement with intrinsic compensation of thermal fluid conductivity, IEEE Sensors Journal 20 (11) (2020) 5698–5704.

[14] D. Kuvshinov, M. Bown, J. MacInnes, R. Allen, R. Ge, L. Aldous, C. Hardacre, N. Doy, M. Newton, G. McHale, Thermal conductivity measurement of liquids in a microfluidic device, Microfluidics and Nanofluidics 10 (1) (2011) 123–132.

[15] S. R. Choi, D. Kim, Measurement of thermal properties of microfluidic samples using laser point heating thermometry, Thermochimica acta 455 (1-2) (2007) 11–15.

[16] M. Gustavsson, H. Nagai, T. Okutani, Thermal effusivity measurements of insulating liquids using microsized hot strip probes, Review of scientific instruments 74 (10) (2003) 4542–4548.

[17] G. V. Casquillas, M. Le Berre, C. Peroz, Y. Chen, J.-J. Greffet, Microlitre hot strip devices for thermal characterization of nanofluids, Microelectronic engineering 84 (5-8) (2007) 1194–1197.

[18] S. R. Choi, J. Kim, D. Kim, 3 ω method to measure thermal properties of electrically conducting small-volume liquid, Review of scientific instruments 78 (8) (2007) 084902.

[19] A. Franco, An apparatus for the routine measurement of thermal conductivity of materials for building application based on a transient hot-wire method, Applied Thermal Engineering 27 (14-15) (2007) 2495–2504.

[20] L. Qiu, Y. Ouyang, Y. Feng, X. Zhang, X. Wang, In vivo skin thermophysical property testing technology using flexible thermosensor-based 3ω method, International Journal of Heat and Mass Transfer 163 (2020) 120550.

[21] S. E. Gustafsson, Transient plane source techniques for thermal conductivity and thermal diffusivity measurements of solid materials, Review of scientific instruments 62 (3) (1991) 797–804.

[22] M. S. Cheri, H. Latifi, J. Sadeghi, M. S. Moghaddam, H. Shahraki, H. Hajghassem, Real-time measurement of flow rate in microfluidic devices using a cantilever-based optofluidic sensor, Analyst 139 (2) (2014) 431–438.

[23] R. Attia, D. C. Pregibon, P. S. Doyle, J.-L. Viovy, D. Bartolo, Soft microflow sensors, Lab on a Chip 9 (9) (2009) 1213–1218.

[24] Q. Wang, Y. Wang, L. Dong, MEMS flow sensor using suspended graphene diaphragm with microhole arrays, Journal of Microelectromechanical Systems 27 (6) (2018) 951–953.

[25] C. Yang, M. Kümmel, et al., A self-heated termistor flowmeter for small liquid flow in microchannels, Sensors and Actuators 15 (1) (1988) 51–62.

[26] C. Clausen, T. Pedersen, A. Bentien, The 3-omega method for the measurement of fouling thickness, the liquid flow rate, and surface contact, Sensors 17 (3) (2017) 552.

[27] G. Oudebrouckx, T. Vandenryt, S. Bormans, P. Wagner, R. Thoelen, Measuring thermal conductivity in a microfluidic device with the transient thermal offset (TTO) method, IEEE Sensors Journal.

[28] C. Gobbé, S. Iserna, B. Ladevie, Hot strip method: application to thermal characterisation of orthotropic media, International Journal of Thermal Sciences 43 (10) (2004) 951–958.

[29] S. E. Gustafsson, E. Karawacki, M. N. Khan, Transient hot-strip method for simultaneously measuring thermal conductivity and thermal diffusivity of solids and fluids, Journal of Physics D: Applied Physics 12 (9) (1979) 1411.

[30] L. Broniarz-Press, K. Pralat, Thermal conductivity of newtonian and non-newtonian liquids, International journal of heat and mass transfer 52 (21-22) (2009) 4701–4710.

[31] Q. Wang, O. Steinbock, Flow-assisted self-organization of hybrid membranes, Chemistry–A European Journal 25 (44) (2019) 10427–10432.

[32] Thermtest. (2020) Materials thermal properties database. [Online]. Available: `https://thermtest.com/materials-database`, retrieved on 2020/04/19.

[33] A. Guimarães, F. Machado, E. Da Silva, A. Mansanares, Thermal effusivity and thermal conductivity of biodiesel/diesel and alcohol/water mixtures, International Journal of Thermophysics 33 (10-11) (2012) 1842–1847.

[34] A. S. Teja, Simple method for the calculation of heat capacities of liquid mixtures, Journal of Chemical and Engineering Data 28 (1) (1983) 83–85.

[35] C. Offenzeller, M. A. Hintermüller, M. Knoll, B. Jakoby, W. Hilber, Simultaneous microfluidic flow velocity and thermal conductivity measurement utilizing screen printed thermal sensors, in: 2019 IEEE SENSORS, IEEE, 2019, pp. 1–4.